

Learnable analysis module for subcellular, time lapse microscopy assays

Samuel V. Alworth, Seho Oh, Yuki Cheng, James SJ Lee

SVision LLC, 3633 136th Pl. SE, Suite 300, Bellevue, WA 98006, USA



Introduction

A new generation of microscope and fluorescent probe technologies has enabled the visualization of subcellular and molecular events in live cell time-lapse microscopy assays. We have previously validated that a subcellular object detection algorithm using confidence maps could achieve highly accurate and robust performance in the synaptic vesicle recycling assay. To generalize the software for additional applications, we have implemented a new "learnable" algorithm architecture. The learning module consists of a generalized algorithm architecture and a teaching user interface for algorithm optimization. The interface allows the user to optimize the algorithm configuration using a drawing tool on images without any image processing knowledge.

We validated the performance of the learning module using time-lapse image sets from an FM dye-based assay of synaptic vesicle recycling, as well as synthetically created time-lapse images. Tests were conducted comparing the new learnable method performance to the validated non-learnable algorithm. We found that the learnable methods can achieve better results than the validated version that is proven to provide significant improvements in synaptic detection sensitivity and specificity, synaptic localization and tau fitting accuracy for both normal and simulated noise conditions over other methods.

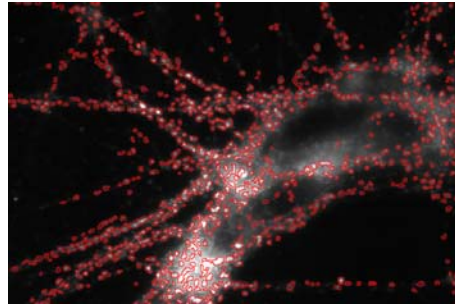


Fig 1. Representative study image showing detected axon terminals using the validated algorithm. It shows excellent performance detecting and segmenting the fluorescently labeled axon terminals, and provides a good baseline for evaluation of the new learning module.

Learnable Detection Method

The learnable detection method generates high confidence detection regions by applying grayscale morphological image processing operations. The morphology operations inherently normalize large intensity fluctuations in images to detect small image features, such as common subcellular phenomena. Morphology based region detection does not introduce phase shift or blurring effect. It is a simple, fast and general method for small object detection in fluorescent images. The new method has two steps; background correction and region partition. It requires only two parameters; one for each of the kernel sizes used in the two steps (described below).

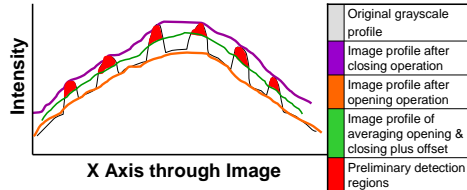


Fig 3. This illustrated example shows how morphology processing performs background correction and enhances small features. A) Applying grayscale morphological closing to the input image to generate the closed image (purple), B) Applying grayscale morphological opening to the input image to generate the opened image (orange), C) generating the offset image by averaging the closed image with the opened image and adding an offset (green), and D) subtracting the offset image from the original image (red regions).

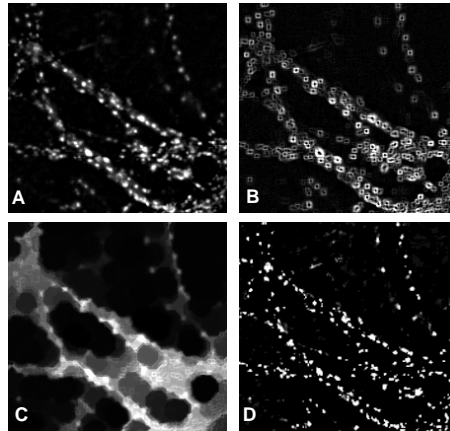


Fig 4. The learnable detection method then performs region partition using morphological dilation. All the example images have been adjusted to enhance their presentation. The corrected image (A) is dilated to generate expanded regions in x,y but with the same intensity peaks as the corrected image. When this image is subtracted from the corrected image it generates region boundaries for the peaks in the corrected image (B). A larger dilation parameter will group neighboring peaks together, while a smaller dilation will separate them. To generate the final confidence map (D) a closing operation is performed on the corrected image, and the partition boundaries are added to it. This image is shown in (C). Image C is subtracted from the corrected image (A) to produce the confidence map (D). The confidence map can be thresholded to produce the final segmentation mask.

Validated Detection Method

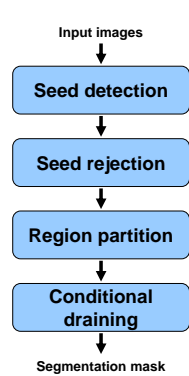


Fig 2. The validated algorithm is an improvement to the standard watershed method. A basic threshold is applied to detect candidate peak points (seeds). Then an iterative flooding operation is performed from the threshold until peak points (seed candidates) are detected. Some seeds are rejected as false alarms if the contrast of the seed and its neighbor pixels is less than a threshold value (default at 768 for 16 bit image). The original mask is partitioned into regions using a labeled zone of interest function about the seed points. The conditional draining step finalizes the segmentation mask region for each axon terminal through iterative draining with area and shape limitations, using the seed points and partition areas as the range.

The approach is difficult to generalize for broad applications because it has many algorithm parameters and is slow.

Teaching Interface

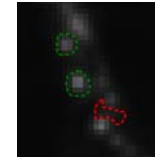
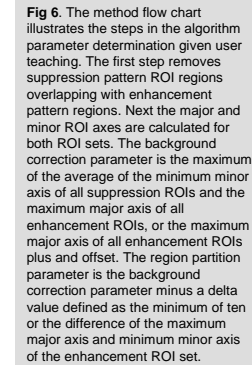


Fig 5. The two parameters required by the learnable detection method can be set by user drawing. Green regions of interest (ROIs) indicate the types of spot patterns desired for enhancement, and red ROIs indicate the patterns for suppression. The learning module maps the size information from these ROIs to configure the two detection method parameters.



Study Materials and Methods

42 images from synaptic vesicle recycling assays using fluorescent FM dye were used for this study. The time-lapse images show the destaining of individual synapses of a small number of rat hippocampal neurons in microisland culture (Fig 1). For this study, only the maximum projection image through the series was used. In addition, for each image, four additional synthetic images were created by adding four levels of zero mean Gaussian noise of standard deviation (sigma) levels 2, 4, 5 and 6. The estimated average signal level for the study images is about 12 grayscale counts, therefore the added noise levels are quite significant. This brings the total study images to 210, with a total of 42,589 labeled objects.

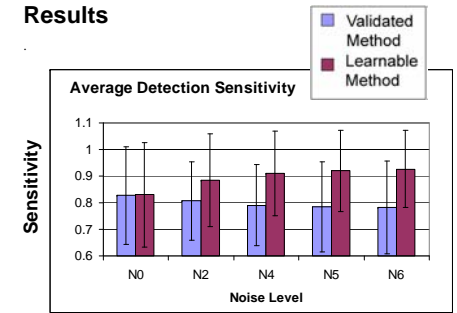
A manual definition of synaptic centers was created and subject to independent review and revision. In total 42,589 true objects were created for the centers using a ROI drawing tool, which was used as a "gold standard truth" for comparing the validated method and new learnable method.

Sensitivity is reported for each method. Sensitivity is defined as the number of correctly detected objects divided by the number of all true objects. The mean and standard deviation of sensitivity is reported for all 210 images.

| Current method result | | Learnable method result | | Total |
|-----------------------|-----|-------------------------|-----|-------|
| SVision Result | A | B | C | D |
| + | a | b | c | a+b+c |
| - | d | e | f | d+e+f |
| Total | a+d | b+e | c+f | 0 |

Fig 7. For statistical evaluation of the relative sensitivity of the two methods, the conditional binomial test¹ is used in a matched pairs study². The two methods are arrayed above. The test is conditional because it depends on the number of discordant pairs, B+C. The conditional binomial test is the McNemar's exact test for testing the quality of discrepant proportions in the matched pairs study design.

Results



| Noise Level | A | B | C | χ^2 | b/c ratio | χ^2 value at alpha = 0.05 |
|-------------|------------|----------|-----------|----------|-----------|--------------------------------|
| N0 | 33532.8684 | 2029.023 | 1090.1079 | 282.6307 | 1.861305 | >> 3.841 |
| N2 | 30439.8919 | 8702.839 | 4491.2445 | 1344.355 | 1.937734 | >> 3.841 |
| N4 | 29012.7364 | 12761.64 | 6701.5772 | 1888.857 | 1.904273 | >> 3.841 |
| N5 | 29105.6482 | 9466.475 | 3001.0406 | 3352.86 | 3.154397 | >> 3.841 |
| N6 | 28589.2021 | 15495.98 | 8460.5443 | 2066.134 | 1.831559 | >> 3.841 |

Fig 8. Study results show that the new learnable method achieves higher level of detection sensitivity of the custom benchmark. The conditional binomial test shows that the relative sensitivity of the new method is statistically greater at the 95% confidence level. Moreover the new method is faster, simpler, can be generalized for broad applications, and can be optimized with a teach by drawing interface.

Future Efforts

- We will continue to modify and improve the performance of the learning module
- We will apply it to new applications

Literature cited

- Lei, X., Davis, D., Kuan, L., Lee, JSJ., Oh, S. 1998. The Conditional Binomial Test Revisited for Clinical Trials. *Journal of Biopharmaceutical Statistics*. 8(4):533-543.
- Breslow, Norman. 1990. Biostatistics and Bayes. *Statistical Science* 5: 269-298

Acknowledgments

This research was supported in part by grant no. 2R44MH075498 from the National Institute of Mental Health